# Parametric potential method for generating atomic data

F. J. Rogers, B. G. Wilson, and C. A. Iglesias
*Lawrence Livermore National Laboratory, University of California, P.O. Box 808, Livermore, California 94550*
(Received 23 May 1988)

It is shown that an analytic effective potential given by a sum of Yukawa terms plus a long-ranged Coulomb tail can provide atomic data (energy levels, oscillator strengths, photoionization cross sections) of accuracy comparable to single-configuration, relativistic, self-consistent-field calculations. The Yukawa terms are weighted by shell occupancy. The screening parameters in the exponentials account for electron shielding of the nuclear charge. Parameter values are obtained by an iterative solution for the eigenvalues of a spin-averaged Dirac equation to match experimental ground-state configuration-averaged ionization energies. The configuration term structure is included by use of Condon-Slater theory. Scaling laws to adjust the screening parameters are given in order to account for multiply excited configurations, inner-core excitations, and the orbital-angular-momentum dependence of excited valence electrons. The method is used to generate prefitted effective potentials for all isoelectronic sequences up to zinc. Comparisons to experimental and self-consistent-field calculations are presented.

## I. INTRODUCTION

The calculation of plasma radiation properties is a complex problem that is currently being readdressed by several groups. This was prompted, in part, by discrepancies between existing theories and observations of the solar neutrino flux,[1] the mass and the period ratios of Cepheids,[2] and analysis of the solar interior through helioseismology,[3] all of which require accurate opacities as input. The development of supercomputing facilities now allows plasma- and atomic-physics details, previously considered prohibitively complex, to be incorporated into opacity calculations. Thus, a new generation of opacity codes will be used to address astrophysics concerns, and the power of the new computers allows freedom in the approach chosen to calculate these opacities. In order to evaluate their relative merits, it is important to know what physics principles are incorporated into each code. This paper documents the atomic physics of the OPAL opacity code[4] being developed by the authors.

The OPAL code uses the method of detailed configuration accounting (DCA), as opposed to an average-atom model.[5] That is, ion stages and the electron configurations of those ions are considered explicitly. In addition, the OPAL code considers the detailed energy level structure of each configuration.

Detailed configuration accounting requires atomic photoabsorption data for all possible transitions from each occupied atomic level. The data in the OPAL code is generated on line by solving a spin-averaged Dirac equation[6] for effective electron-ion potentials. This approach is feasible because it is possible to quickly produce simple parametrized analytic potentials that yield atomic data of accuracy comparable to single-configuration Hartree-Fock potentials (including relativistic corrections) for all configurations of all ions of light elements. In this work we are primarily interested in obtaining data for the calculation of astrophysical opacities, i.e., complete data for all materials having atomic number $Z$ less than 31. However the methods presented here should be reliable up to at least $Z=40$.

By comparison, the atomic data to be utilized by other opacity projects[7-11] are isolated-atom results that are precalculated and retrieved as necessary. The opacity project of Refs. 9–11 will employ close-coupling calculations that produce very accurate *ab initio* data,[12-17] while Huebner and co-workers[7,8] will use empirical fits[18,19] to energy levels and transition strengths (generated from the Cowan structure code) for fast retrieval.

Our approach was chosen because stored or prefitted data may constrain calculations to regions of low density where isolated-ion data are adequate. By generating data on line, density effects on the wave functions may be incorporated as needed by screening the long-ranged Coulomb tail of isolated ions. A useful feature of our approach is that it provides the ability to study easily the effects of atomic physics issues on the opacity by simply adjusting the atomic physics computer package. Such issues include the relative importance of term splitting and the introduction of intermediate coupling.

## II. EFFECTIVE POTENTIALS

In the past it has been shown that experimental atomic properties can be well represented by independent-particle models[20] and that optimized potentials yield wave functions which are almost the same as Hartree-Fock wave functions.[21,22] In addition, they provide a natural solution for extending results of Hartree-Fock quality to excited states.

For atomic valence electrons, two-parameter effective potentials have been used[23] successfully for energy level calculations,[24-26] elastic-scattering cross sections,[27,28] oscillator strengths,[29,30] and electron impact excitation cross sections.[31,32]

 

Klapisch[33] has used an analytic effective potential involving Yukawa terms modified by polynomials and advocated adjusting parameters in a least-squares sense to reproduce experimental data or *ab initio* calculations. However, all parameters in the potential were optimized and no simple fittings to the parameters resulted. A parametrization similar to Kaplisch's has been postulated by approximating the Hartree-Fock set of equations in momentum space with a local operator.[34]

Analytical effective potentials using variants of the Yukawa form have also been used by Daudey and Berondo,[35] who determined parameters by minimizing the calculated total energy of the atom. The effective potential of Salvat *et al.*[36] is in the form of a Hartree-plus-Slater exchange potential with the local density approximated by Yukawa terms. Both studies were for neutral atoms and no simple fitting of the parameters was given.

In the present work we are interested in finding effective potentials for arbitrary configurations and ion stages. In particular, we will develop a procedure for calculating a large and varied amount of data from a relatively small number of prefitted parameters. Reasonable physically motivated corrections to the parameters are used to extend results to regions where there are no reliable experimental measurements such as density effects and highly ionized ions.

When discussing the effective potentials in OPAL, it is convenient to define the electron configurations as having two components. The first component is a "parent" configuration consisting of all the electrons in a given configuration except one. The excluded electron defines the second component or "running" electron. The parent configuration defines the effective potential for all the subshells available to the running electron. In order to incorporate the shell structure of the parent while retaining an analytic Fourier transform, Rogers[37] introduced a potential with one Yukawa term for each occupied shell in the parent configuration,

$$V=-\frac{2}{r}\left[(Z-\nu)+\sum_{n=1}^{n^*}N_n e^{-\alpha_n r}\right] \tag{1}$$

(in Rydbergs), where

$$\nu=\sum_{n=1}^{n^*}N_n \tag{2}$$

is the number of electrons for the parent ion, $N_n$ the number of electrons in the shell with principal quantum number $n$, $n^*$ the maximum value of $n$ for the parent configuration, and $\alpha_n$ the screening parameter for electrons in shell $n$. As will be shown, a potential of this form is well suited for our purpose.

The screening parameters in Eq. (1) are determined by iteratively solving a spin-averaged Dirac equation and matching the eigenvalues to the experimentally observed one-electron ionization energies. This empirical approach implicitly incorporates electron correlations and other effects (i.e., spin–other-orbit interactions, etc.) which may be neglected in *ab initio* calculations.

Before proceeding with a description of the method, it is useful to discuss specific examples. Consider the configuration $1s^2 2s^2 2p^4$. For the ionization energy of the $2p$ electron, the system is defined by the parent $1s^2 2s^2 2p^3$ plus a running electron. In fact, this parent describes all transitions of the form

$$1s^2 2s^2 2p^3 n_1 l_1 \rightarrow 1s^2 2s^2 2p^3 n_1' l_1' ,$$

where $n_1 l_1$ and $n_1' l_1'$ denote the set of orbitals $2p,3s,3p,\ldots$, including scattering states, so that photoionization and bremsstrahlung can also be considered. Similarly, the parent $1s^2 2s 2p^4$ describes transitions of the form

$$1s^2 2s 2p^4 n_2 l_2 \rightarrow 1s^2 2s 2p^4 n_2' l_2' ,$$

where now the set $n_2 l_2$ and $n_2' l_2'$ includes the $2s$ orbital.

Now, if we assign $n_1 l_1 = 2p$ and $n_2 l_2 = 2s$ in the previous examples, then the initial configurations are identical. The OPAL code uses different effective potentials because the parent configurations are different. In contrast, a self-consistent-field (SCF) potential uses the same set of orbital wave functions for the initial configurations in both types of transitions. Each of the final configurations would then be computed in separate SCF calculations.

It should be clear then that the effective potential in OPAL is not an independent-particle parametrization of a SCF potential. In the latter the configuration-averaged energy is constructed from interacting electrons using single-particle eigenvalues and Slater integrals[38] and the transition energies are given by differences in total energies. In OPAL, transition energies are assumed to be differences between the eigenvalues of the running electron. The eigenvalues of the parent-configuration closed shells have no physical content. In contrast, the interpretation of Hartree-Fock eigenvalues as ionization energies (neglecting core relaxation) is a consequence of Koopmans's theorem.[39]

## III. INFLUENCE OF ELECTRONIC STRUCTURE ON EFFECTIVE POTENTIALS

### A. Ground-state parents

In this section we describe our method for single-electron transitions involving a parent configuration consisting of a closed core plus an open valence subshell. These will be referred to in this paper as ground-state parents. They are the most basic parent configurations, since results from the ground-state parents are used to generate effective potentials for core electrons and multiply excited configurations. Standard "speedometer" ordering of subshells ($1s,2s,2p,3s,3p,3d,\ldots$) is assumed. With the exception of some neutral and singly ionized elements, this ordering corresponds to the energetically lowest configuration having up to 37 bound electrons. Effective potentials for configurations out of speedometer order are described later.

Screening parameters are obtained systematically for varying nuclear charge in each isoelectronic ground-state parent configuration. Starting with two electron ions (i.e., one-electron parents), a spin-averaged Dirac equation[6] was solved iteratively to find the screening parame-

ter for the $K$ shell, $\alpha_k$, that reproduces experimental ground-state ionization energies. The $\alpha_k$ parameter was similarly determined for two-electron parents. For three-electron parents, which require a $K$- and $L$-shell parameter, the $K$-shell parameter was fixed at the two-electron parent value. For this and subsequent isoelectronic series, only the outermost-shell parameter was optimized, all other inner-shell parameters being frozen at their noble gas parent configuration values. Various sources were used for the experimental energies.[40–48]

It was found that each shell parameter could be fitted very accurately along an isoelectronic sequence with the simple form

$$\alpha_n=(\xi_n+1)\sum_{j=0}^{3}\frac{a_j(\nu_n)}{\xi_n^j}\ . \tag{3}$$

Each $\alpha_n$ is fitted by coefficients which depend on the occupancy of the parent up to that shell,

$$\nu_n=\sum_{n=1}^{n}N_n \tag{4}$$

and by the net charge at the shell

$$\xi_n=Z-\nu_n \tag{5}$$

for the parent-configuration ion.

In Table I we present a compilation of the coefficients $a_j$. There are two modifications to the results previously given by Rogers.[37] For parents with $M$-shell electrons, the number of coefficients was increased to four. This was necessary since the larger number of electrons requires very accurate fits to the screening parameters. Secondly, the true ionization energies were not used as in Ref. 37, but rather the configuration-average energy difference between speedometer-ordered ground-state configurations of two adjacent ion stages were used. The latter differs from the ground-state energy when there is appreciable level splitting about the configuration average or when the speedometer order does not yield the energetically lowest configuration. The true ionization energy (the energy to the actual ground state of the next ion stage) can be calculated by adding offsets to the quasi-ionization energies. Along any isoelectric sequence these offests are nearly linear in $Z$ (with the exception of neutral elements) and so can be obtained from the data in Table II.

The quality of the parametric fit is illustrated for the silicon isoelectronic sequence in Table III. The data represent true ionization energies. A second example is afforded by the isoelectronic sequence (closed shells)

TABLE I. Coefficients for the screening parameter fits, Eq. (3).

| $n$ | $\nu_n$ | Parent configuration | $a_0$ | $a_1$ | $a_2$ | $a_3$ |
|---|---|---|---|---|---|---|
| 1 | 1 | $1s$ | 1.2929 | −0.5110 | 0.2881 | |
| | 2 | $1s^2$ | 0.8855 | 0.2549 | −0.0901 | |
| 2 | 3 | $2s$ | 0.2781 | −0.0109 | 0.0275 | |
| | 4 | $2s^2$ | 0.2602 | 0.2755 | −0.1445 | |
| | 5 | $2s^2 2p$ | 0.3056 | 0.3228 | −0.1269 | |
| | 6 | $2s^2 2p^2$ | 0.3092 | 0.5368 | −0.2403 | |
| | 7 | $2s^2 2p^3$ | 0.3345 | 0.6294 | −0.2524 | |
| | 8 | $2s^2 2p^4$ | 0.3242 | 0.8749 | −0.3855 | |
| | 9 | $2s^2 2p^5$ | 0.3448 | 0.9838 | −0.4094 | |
| | 10 | $2s^2 2p^6$ | 0.3386 | 1.1323 | −0.4904 | |
| 3 | 11 | $3s$ | 0.1030 | 0.6546 | −1.1826 | 0.6691 |
| | 12 | $3s^2$ | 0.1064 | 0.4699 | −0.5769 | 0.2794 |
| | 13 | $3s^2 3p$ | 0.1259 | 0.4485 | −0.4154 | 0.1705 |
| | 14 | $3s^2 3p^2$ | 0.1207 | 0.5551 | −0.4708 | 0.1754 |
| | 15 | $3s^2 3p^3$ | 0.1392 | 0.5727 | −0.4249 | 0.1444 |
| | 16 | $3s^2 3p^4$ | 0.1375 | 0.6759 | −0.4922 | 0.1617 |
| | 17 | $3s^2 3p^5$ | 0.1328 | 0.8365 | −0.7315 | 0.2950 |
| | 18 | $3s^2 3p^6$ | 0.1437 | 0.9129 | −0.6940 | 0.2503 |
| | 19 | $3s^2 3p^6 3d$ | 0.1499 | 0.9801 | −0.7762 | 0.2340 |
| | 20 | $3s^2 3p^6 3d^2$ | 0.1541 | 1.0467 | −0.8750 | 0.3072 |
| | 21 | $3s^2 3p^6 3d^3$ | 0.1616 | 1.1131 | −0.9604 | 0.3607 |
| | 22 | $3s^2 3p^6 3d^4$ | 0.1625 | 1.1833 | −1.0028 | 0.3754 |
| | 23 | $3s^2 3p^6 3d^5$ | 0.1659 | 1.2700 | −1.0919 | 0.4147 |
| | 24 | $3s^2 3p^6 3d^6$ | 0.1613 | 1.3783 | −1.2139 | 0.4793 |
| | 25 | $3s^2 3p^6 3d^7$ | 0.1682 | 1.4502 | −1.2701 | 0.5008 |
| | 26 | $3s^2 3p^6 3d^8$ | 0.1720 | 1.4939 | −1.2467 | 0.4758 |
| | 27 | $3s^2 3p^6 3d^9$ | 0.1714 | 1.5546 | −1.2111 | 0.4256 |
| | 28 | $3s^2 3p^6 3d^{10}$ | 0.1726 | 1.7227 | −1.5856 | 0.6383 |
| | 29 | $4s$ | 0.0597 | 0.5385 | −0.4503 | 0.1419 |

TABLE II. Offsets values ($cm^{-1}$) for physical ionization energies of isoelectronic sequences with $N$ bound electrons. Shifts for sequences not present are assumed zero. Offsets for higher ion stages can be obtained by linear extrapolation of ion stages $+1$ and $+2$.

| $N$ | Ion stage 0 | $+1$ | $+2$ |
|---|---|---|---|
| 7 | 7313 | 9703 | 12 118 |
| 8 | 25 543 | 32 509 | 39 122 |
| 9 | 10 157 | 12 720 | 15 488 |
| 15 | 4498 | 5761 | 7053 |
| 16 | 14 776 | 17 995 | 21 060 |
| 17 | 6430 | 7217 | 8631 |
| 18 | 477 | 722 | 1033 |
| 21 | 10 098 | 7308 | 9374 |
| 22 | 11 570 | 15 054 | 18 848 |
| 23 | 20 500 | 25 016 | 36 082 |
| 24 | 33 046 | 44 106 | 53 295 |
| 25 | 37 692 | 29 328 | 33 698 |
| 26 | 18 560 | 20 539 | 24 500 |

$3s^23p^63d^3$ given in Table IV. With the exception of the first two elements ($Z=21$ and 22), this configuration is the physical ground-state configuration for the scandium isoelectronic sequence. For these two elements the energetically lower configurations may be computed in the same manner as excited parent configurations (to be described later).

Experimental energy levels of excited running electrons from the same parent but with a different angular-momentum label $l$ have different ionization limits. The effective potential obtained from Table I should be expected to fit excited states where the running electron is of the same $l$ as the ground-state configuration. For accuracy one could fit an effective potential to the lowest state of each ionization limit, that is, generate $l$-dependent effective potentials. (Note that properties of the spherical harmonics ensure wave-function orthogonality.) However, it was found that a simple correction factor to the valence shell parameter of the form

TABLE III. Comparison of the ground-state $3p$ electron configuration-average ionization energy (Ry) for the silicon isoelectronic sequence.

| $Z$ | Experiment | OPAL | % difference |
|---|---|---|---|
| 14 | 0.5698 | 0.5721 | +0.40 |
| 15 | 1.4146 | 1.4198 | +0.37 |
| 16 | 2.5280 | 2.5164 | −0.46 |
| 17 | 3.8653 | 3.8587 | −0.17 |
| 18 | 5.4376 | 5.4359 | −0.03 |
| 19 | 7.2416 | 7.2433 | +0.02 |
| 20 | 9.2446 | 9.2789 | +0.37 |
| 22 | 13.9746 | 14.0309 | +0.40 |
| 24 | 19.7193 | 19.6883 | −0.16 |
| 26 | 26.2835 | 26.2514 | −0.12 |
| 27 | 29.9138 | 29.8730 | −0.14 |

TABLE IV. Comparison of the ground-state $3d$ configuration-average ionization energy (Ry) for the isoelectronic sequence $1s^22s^22p^63s^23p^63d^3$.

| $Z$ | Experiment | OPAL | % difference |
|---|---|---|---|
| 21 | 0.2187 | 0.2188 | +0.05 |
| 22 | 0.9590 | 0.9621 | +0.32 |
| 23 | 2.1132 | 2.0997 | −0.64 |
| 24 | 3.5396 | 3.5434 | +0.10 |
| 25 | 5.2407 | 5.2483 | +0.15 |
| 26 | 7.1819 | 7.1970 | +0.21 |
| 27 | 9.3587 | 9.3818 | +0.25 |
| 28 | 11.8374 | 11.7986 | −0.33 |
| 30 | 17.3141 | 17.3198 | +0.03 |
| 34 | 31.1015 | 31.0883 | −0.04 |

$$\alpha' = \alpha\tau \ ,$$

with

$$\tau = 1 + \Theta(n_v)[l(l+1) - l_v(l_v+1)] \ , \tag{6}$$

can account for most of the $l$ dependence. Here, $n_v$ and $l_v$ are the principal and orbital quantum labels of the valence subshell, respectively, and $l$ is the orbital label of the running electron. [In Eq. (6) and throughout the paper, the unprimed $\alpha$'s refer to the screening parameter obtained directly from Eq. (3) and Table I.] The factor $\tau$ is applied only for those $l$ greater than $l_v$. Empirical fits to the shell-dependent scaling factor $\Theta$ are listed in Appendix A.

As an illustration, consider carbonlike oxygen in the ground-state configuration $1s^22s^22p^2$. The $K$- and $L$-shell screening parameters given by Eqs. (3)–(5) are 6.4784 and 1.5964, respectively, for all excited configurations of the form $[\mathrm{Be}]2p^1ns$ and $[\mathrm{Be}]2p^1np$. Using Eq. (6) for configurations $[\mathrm{Be}]2p^1nd$, the $L$-shell parameter becomes 1.7560, for $[\mathrm{Be}]2p^1nf$ it is 1.9954, etc. A comparison of experimental and calculated configuration-average ionization energies for several configurations of carbonlike oxygen is given in Table V. A similar comparison for neutral silicon is presented in Table VI. In general, the

TABLE V. Configuration-average ionization energies (Ry) for the outermost electron of carbonlike oxygen. Only open subshells are identified.

| Configuration | Experiment | OPAL | % error |
|---|---|---|---|
| $2p^2$ | 3.9497 | 3.9649 | +0.4 |
| $2p3p$ | 1.3234 | 1.3267 | +0.2 |
| $2p4p$ | 0.6814 | 0.6863 | +0.7 |
| $2p3s$ | 1.5883 | 1.5675 | −1.3 |
| $2p4s$ | 0.7818 | 0.7733 | −1.1 |
| $2p5s$ | 0.4632 | 0.4612 | −0.4 |
| $2p3d$ | 1.0560 | 1.0633 | +0.7 |
| $2p4d$ | 0.5852 | 0.5909 | +1.0 |
| $2p5d$ | 0.3723 | 0.3748 | +0.7 |

TABLE VI. Configuration-average ionization energies (Ry) for the outermost electron in neutral silicon. Only open subshells are identified.

| Configuration | Experiment | OPAL | % error |
|---|---|---|---|
| $3p^2$ | 0.569 83 | 0.572 10 | +0.4 |
| $3p4p$ | 0.154 71 | 0.155 11 | +0.3 |
| $3p5p$ | 0.076 85 | 0.079 11 | +2.9 |
| $3p4s$ | 0.233 40 | 0.231 91 | −0.6 |
| $3p5s$ | 0.102 16 | 0.101 81 | −0.3 |
| $3p6s$ | 0.057 32 | 0.056 04 | −2.3 |
| $3p3d$ | 0.130 15 | 0.125 34 | −3.6 |
| $3p4d$ | 0.071 37 | 0.069 51 | −2.7 |

agreement remains good for most ion stages of most elements. Loss of accuracy can occur for high Rydberg states of some elements as small discrepancies in total energies correspond to appreciable relative errors in the ionization energies. This difficulty is also present in SCF calculations as illustrated in Table VII for neutral argon.

### B. Excited parent configurations

Ground-state parent configurations and a running electron comprise only a small subset of all transitions that must be considered in an opacity calculation. In this section we show how the effective potential for excited parent configurations can be generated from the results for the ground-state parent configuration using simple scaling laws. The scaling laws depend on the manner in which the excited parent configuration is generated from the ground-state parent configuration by single-electron excitations. These excitations fall into two classes: (1) those within the valence shell of the ground-state parent configuration and (2) those involving shell occupancy redistribution. Such a distinction could probably have been avoided if we had characterized our effective potential by a Yukawa term for each subshell. However, such an approach unnecessarily complicates an efficient and simple scheme by proliferating the number of parameters to be fitted.

We begin with excited parent configurations involving only promotions within the valence shell. For example, consider transitions of the form

$$[\cdots]2s2p^2nl \rightarrow [\cdots]2s2p^2n'l' ,$$

where $[\cdots]$ indicates closed subshells. These transitions involve the parent $[\cdots]2s2p^2$, which can be generated by promoting a $2s$ electron from the ground-state parent to a $2p$ orbital. The transition energies arising from these parents are very similar to those of the ground-state parent, but if the differences are of the order of the linewidth or greater, these differences can make an important contribution to the opacity. The promotion does not involve a redistribution of the parent shell occupancy, so only the valence shell screening parameter needs adjustment. The following scaling law has been found to work well:

$$\alpha'_L = \alpha_L \tau \bar{r} . \tag{7}$$

Here, $\alpha_L$ is the screening parameter of the ground-state parent (from Table I) when the running electron occupies its lowest possible orbital (in this example the $2p$ orbital), and $\tau$ is defined in Eq. (6). The factor

$$\bar{r} = \frac{\sum_l N^g_{nl} r_{nl}}{\sum_l N^e_{nl} r_{nl}} \tag{8}$$

is the ratio of the weighted locations of the outermost radial wave function amplitude maxima $r_{nl}$, obtained by solving the spin-averaged Dirac equation for the effective potential corresponding to the ground-state parent. The sum is over the subshells of the parent-configuration valence shell and the weights $N^g_{nl}$ and $N^e_{nl}$ denote the occupancies of the subshells in the ground- and excited-state parent configurations, respectively. This ansatz is motivated by considering the effect of charge redistribution in an SCF calculation.

In this example the new $L$-shell screening parameter describes excited parent configurations where the running electron is of the same $l$ as its lowest possible orbital. The previously introduced $l$-dependent factor, Eq. (6), again accounts for differing ionization limits.

TABLE VII. Configuration-average ionization energies (Ry) for the outermost electron in neutral argon. The Cowan SCF results are also presented. Only open subshells are identified.

| Configuration | Expt. | Cowan | % error | OPAL | % error |
|---|---|---|---|---|---|
| $3p^6$ | 1.158 31 | 1.147 83 | −0.9 | 1.161 75 | 0.3 |
| $3p^5 4p$ | 0.190 24 | 0.195 90 | +2.9 | 0.191 13 | 0.5 |
| $3p^5 5p$ | 0.087 48 | 0.091 86 | +5.0 | 0.092 47 | 5.7 |
| $3p^5 6p$ | 0.049 47 | 0.053 79 | +8.2 | 0.053 02 | 11.2 |
| $3p^5 4s$ | 0.301 92 | 0.305 83 | +1.3 | 0.303 29 | 0.5 |
| $3p^5 5s$ | 0.119 42 | 0.122 77 | +2.8 | 0.120 26 | 0.71 |
| $3p^5 6s$ | 0.063 06 | 0.066 97 | +6.2 | 0.062 30 | 1.2 |
| $3p^5 3d$ | 0.123 05 | 0.124 41 | +1.1 | 0.126 18 | 2.5 |
| $3p^5 4d$ | 0.067 39 | 0.069 71 | +3.4 | 0.071 30 | 5.8 |
| $3p^5 5d$ | 0.040 87 | 0.044 03 | +7.7 | 0.044 96 | 10.0 |

Figure 1 plots the ionization potential for $2p$ electrons leaving a $[\cdots]2s2p$ parent and also for leaving a $[\cdots]2p^2$ parent. Values are given relative to the ionization energy for a $2p$ electron leaving a $[\cdots]2s^2$ parent. Results from Eqs. (7) and (8) are compared with experimental values for varying nuclear charge. Except for nearly neutral ions, these incremental ionization energies scale linearly with the net charge and also with the number of electrons excited within the parent.[49] The scaling procedure tracks the experimental result fairly well, but we have found that nearly exact agreement can be obtained by modifying Eq. (7) with the factor $\sigma$ according to

$$\alpha'_L=\alpha_L[1+(\bar{r}-1)\sigma] , \tag{9}$$

which was fitted for different isoelectronic sequences by the form

$$\sigma=C_0+G/(1+Z-\nu) . \tag{10}$$

Values of $C_0$ and $G$ are listed in Appendix B.

Experimental data for the $M$ shell is limited, but for the parent promotion $3s^2\rightarrow 3s3p$ shown in Fig. 1 the situation is somewhat different than it is for the $L$ shell. Introducing the additional scale factor in Eq. (9) does not improve agreement. In contrast to the $L$ shell, where values for $r_{2s}$ and $r_{2p}$ differ appreciably, in the $M$ shell they are nearly equal. In fact, $r_{3p}$ becomes greater than $r_{3s}$ near neutrality, consistent with the increased ionization potential (i.e., positive value for the incremental ionization energy plotted). The adjustment factor in Eq. (9) may be added for $M$-shell cases where the value of Eq. (8) differs appreciably from unity, that is, for parent configurations involving $s$ and $p$ electrons promoted to the $d$ shell. Unfortunately, experimental data to determine $\sigma$ are insufficient.

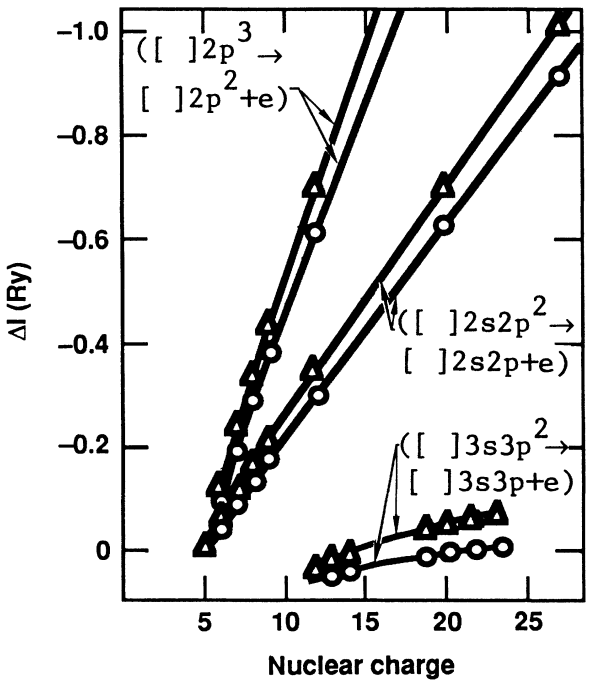


FIG. 1. Comparison of one-electron ionization energies to experiment for excited parent configurations with promotions within the valence shell using Eq. (8) for the scaling: ○, OPAL; △, experiment.

Comparisons of energies for configurations arising from three excited parents of boronlike magnesium in Table VIII typify results from the scaling procedure. Included in the table are results from single-configuration HXR calculations[50] obtained with the Cowan suite of codes[51] and, when available, experiment.[41] Energies are referenced to the parent of the running electron. Energy differences between excited parents (required for equation of state purposes only, since all radiative transitions occur from a common parent; see Sec. IV) are obtained in OPAL from eigenvalues of higher ion stages (see Appendix C).

The second class of promotions, excited configurations involving shell occupancy redistribution of the parent configuration, fall into three categories. In the first category a parent configuration is generated by exciting a core shell electron into the valence shell. For example, from the ground-state silicon parent configuration $1s^22s^22p^63s^23p$ a $K$ shell electron can be promoted, resulting in the excited parent configuration $1s^12s^22p^63s^23p^2$. Now the running electron can occupy the $1s,3p,3d,4s,\ldots$, etc. orbitals. In principle, the screening parameters for all three occupied shells should be adjusted. However, the largest effect is in those shells that undergo a direct change in occupation and these are the only ones we modify. For the $K$ shell in this example, the occupancy is reduced by one and the net $K$-shell charge is increased by one:

$$\alpha_k=(\xi'_k+1)\sum_{j=0}^{3}\frac{a_j(\nu'_k)}{(\xi'_k)^j} , \tag{11}$$

TABLE VIII. Configuration-average energies (Ry) for boronlike magnesium. Only open subshells are identified.

| Configuration | OPAL | Cowan | Experiment |
|---|---|---|---|
| $2s2p2$ | 1.9444 | 1.7890 | 1.9246 |
| $2p3$ | 4.2221 | 4.1489 | 4.3100 |
| $2s^23s$ | 11.1506 | 11.1216 | 11.0326 |
| $2s^23p$ | 11.6532 | 11.7381 | |
| $2s^23d$ | 12.1816 | 12.2357 | 12.1733 |
| $2s^24s$ | 15.0771 | 15.0776 | 15.0168 |
| $2s^24p$ | 15.2800 | 15.3184 | |
| $2s^34d$ | 15.4842 | 15.5077 | 15.4353 |
| $2s2p3s$ | 10.8758 | 10.7531 | 10.7530 |
| $2s2p3p$ | 11.3878 | 11.3276 | |
| $2s2p3d$ | 11.9053 | 11.8192 | |
| $2s2p4s$ | 14.7571 | 14.6638 | |
| $2s2p4p$ | 14.9636 | 14.8926 | |
| $2s2p4d$ | 15.1633 | 15.0796 | |
| $2p^23s$ | 10.5791 | 10.4113 | |
| $2p^23p$ | 11.1011 | 10.9393 | |
| $2p^23d$ | 11.6010 | 11.4241 | |
| $2p^24s$ | 14.4162 | 14.2757 | |
| $2p^24p$ | 14.6267 | 14.4912 | |
| $2p^24d$ | 14.8199 | 14.6758 | |

where $\nu'_k=\nu_k-1=1$ and $\xi'_k=\xi_k+1=13$. The $L$-shell screening parameter is left unchanged from the ground-state parent, so that

$$\alpha_L=(\xi_L+1)\sum_{j=0}^{3}\frac{a_j(\nu_L)}{\xi_L^j}\ , \tag{12}$$

where $\nu_L=10$ and $\xi_L=4$. To a first approximation, except for the direct scaling factor $\xi_L+1$, the $M$ shell looks like phosphoruslike sulfur. Intuitively, this is because the $M$ shell is occupied as in phosphorus and the increased charge of sulfur reflects the fact that the inner-shell vacancy draws the charge density towards the nucleus. Using this physical picture as a guide we calculate $\alpha_M$ according to

$$\alpha_m=(\xi_m+1)\sum_{j=0}^{3}\frac{a_j(\nu'_m)}{(\xi'_m)^j}\ , \tag{13}$$

where $\nu'_M=\nu_m+1=14$ and $\xi'_m=\xi_m+1=2$. A double promotion would be calculated using sulfurlike chlorine parameters for the terms in the sum. The angular-momentum correction factor, Eq. (6), is also included to model series regularities.

Figure 2 gives results comparing calculated $2s$ binding energies for neutral atoms with experiment.[52–54] It is interesting to note that the errors seem to correspond with the error obtained from Cowan's code (but opposite in sign). Table IX compares inner-shell energies for various ions of iron with those calculated from Cowan.

A second category consists of excited parent configurations formed by promoting an inner-shell electron to an unoccupied shell. An example is the silicon parent configuration $1s2s^22p^63s^23p4d$. The $K$- and $L$-shell parameters are computed as in the previous case,

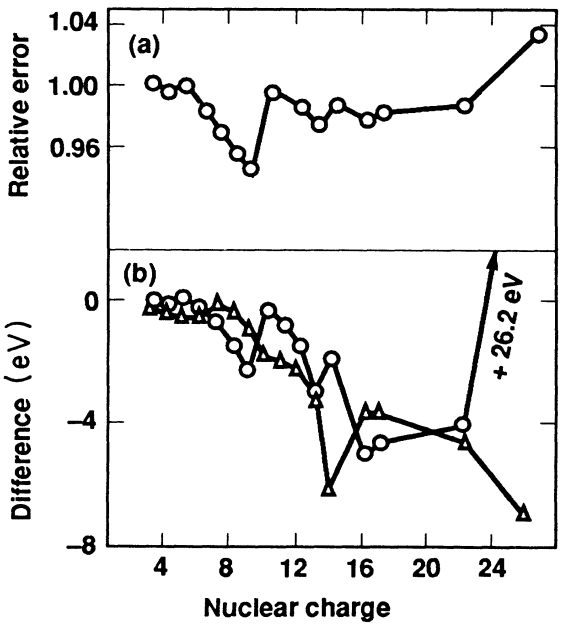


FIG. 2. $2s$ electron binding energy for neutral atoms: (a) relative error for OPAL vs experiments, and (b) energy difference from experiment in eV; ○, OPAL; △, Cowan.

TABLE IX. Comparison of inner-shell ionization energies (eV) with Cowan for various ion stages of iron. The Cowan results are printed directly below those from OPAL. Only open subshells are identified.

| Photoelectron | $3d^8$ | $3d^7$ | $3d^6$ | $3d^5$ | $3d^4$ | $3d^3$ | $3d^2$ | $3d$ | $3p^6$ | $3p^5$ | $3p^4$ | $3p^3$ | $3p^2$ | $3p$ |
|---|---|---|---|---|---|---|---|---|---|---|---|---|---|---|
| $1s$ | 7070 | 7122 | 7145 | 7156 | 7180 | 7235 | 7272 | 7298 | 7322 | 7362 | 7404 | 7442 | 7506 | 754 |
| | 7120 | 7137 | 7156 | 7178 | 7202 | 7239 | 7261 | 7294 | 7329 | 7351 | 7414 | 7459 | 7506 | 755 |
| $2s$ | 879 | 887 | 896 | 905 | 926 | 971 | 1002 | 1031 | 1051 | 1092 | 1124 | 1174 | 1230 | 127 |
| | 850 | 865 | 884 | 912 | 932 | 961 | 992 | 1026 | 1062 | 1100 | 1139 | 1179 | 1221 | 126 |
| $2p$ | 757 | 763 | 771 | 778 | 799 | 836 | 867 | 896 | 920 | 959 | 999 | 1037 | 1093 | 113 |
| | 745 | 728 | 748 | 776 | 796 | 825 | 856 | 890 | 927 | 964 | 1003 | 1044 | 1086 | 113 |
| $3s$ | 95 | 116 | 125 | 147 | 168 | 192 | 216 | 247 | 270 | 299 | 328 | 354 | 393 | 42 |
| | 99 | 113 | 130 | 152 | 173 | 197 | 223 | 250 | 278 | 297 | 334 | 363 | 393 | 42 |
| $3p$ | 59 | 69 | 88 | 110 | 131 | 154 | 178 | 209 | | | | | | |
| | 60 | 74 | 91 | 110 | 132 | 155 | 180 | 206 | | | | | | |

Eqs. (11)–(13). Accordingly, the $M$-shell parameter is calculated using the ground-state parent but scaled with an increased parent charge to account for the $K$-shell vacancy. The remaining $N$-shell parameter is obtained by scaling the $M$-shell parameter of the ground-state parent configuration by the formula

$$\alpha_N = \alpha_M \frac{R_g}{R_e} , \tag{14}$$

using the radial wave functions already calculated for the ground-state parent. In Eq. (14) $R_g$ and $R_e$ are the locations of the last amplitude maxima of the outermost orbital of the ground-state parent ($3p$) and outermost occupied orbital of the excited parent configuration ($4d$), respectively. Again this procedure models the effect of charge redistribution in an SCF calculation. Empirically, it is found that both the $M$-shell and singly occupied outer-$N$-shell parameters must be modified by the angular-momentum factor, Eq. (6), to model series regularities.

The last category of excited parent configurations is formed by simple excitations out of the valence shell. These are commonly referred to as doubly excited states. For neutral silicon an example would be the $1s^2 2s^2 2p^6 3s^2 4f$ parent configuration. The $K$- and $L$-shell parameters remain unchanged from the ground-state parent configuration, while the $M$ shell is computed as if it were the next lightest element,

$$\alpha_m = (\xi'_m + 1) \sum_{j=0}^{3} \frac{a_j(\nu'_m)}{(\xi'_m)^j} , \tag{15}$$

where $\nu'_m = \nu_m - 1 = 12$ and $\xi'_n = Z - \nu'_n = \xi + 1 = 2$. The $N$-shell parameter is calculated as in the second category,

$$\alpha_n = \alpha_m \frac{R_{3p}}{R_{4f}} . \tag{16}$$

Again, $l$ dependence of the screening parameter is included through the factor $\tau$ in Eq. (6).

The rules just described do a good job of calculating atomic data involving excited parents. At the expense of a little added complexity, the procedure can be further refined. This is discussed in Appendix D.

Although each case has been illustrated using a specific example, the generalization to arbitrary configurations should be apparent. Since all fitting and scaling is done using Table I and the wave functions for the ground-state parent, the procedures developed here are independent of the path taken to obtain a given parent excitation. It is important to stress that a large number of electron ionization energies are accurately obtained using effective potentials which are generated from a relatively small data set and scaling procedures. This has made possible on-line computation of all atomic data needed for astrophysical calculations.

## IV. TRANSITION STRENGTHS AND DETAILED STRUCTURE

To obtain reasonable agreement with spectral data, it is necessary to consider the term structure of configurations. In OPAL, configuration structure is calculated in the single-configuration approximation of the Slater-Condon theory of atomic structure.[6] All results in this section assume the $LS$ or Russell-Saunders coupling scheme.[6] The term energies can be obtained using Racha algebra and involve Slater integrals which in turn depend on the set of radial wave functions, $\{\Psi_{nl}\}$, computed from the effective potentials.[55]

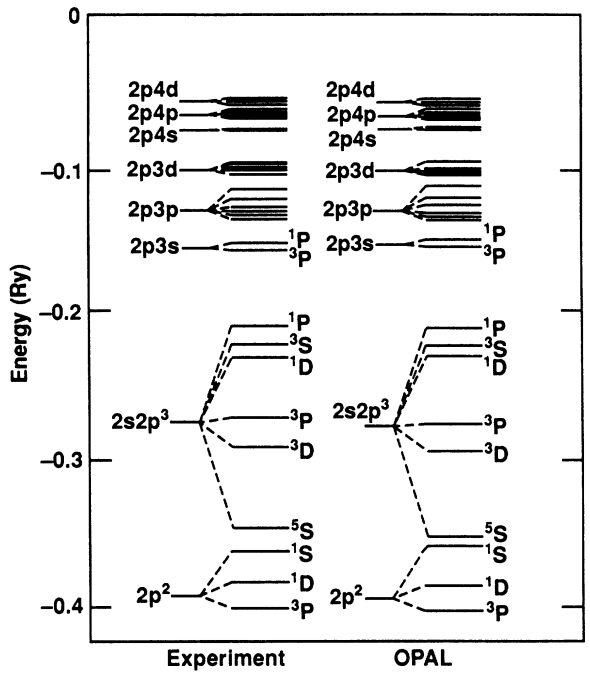


FIG. 3. Comparison of the configuration term structure for carbonlike oxygen.

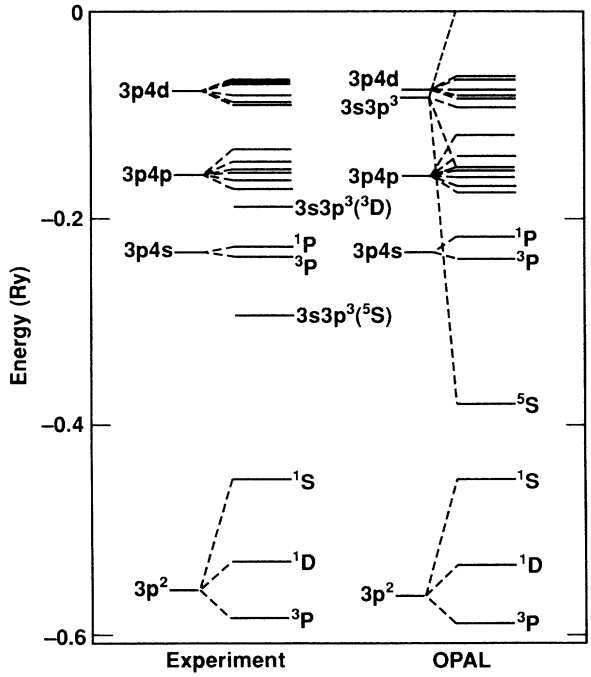


FIG. 4. Comparison of the configuration term structure for neutral silicon.

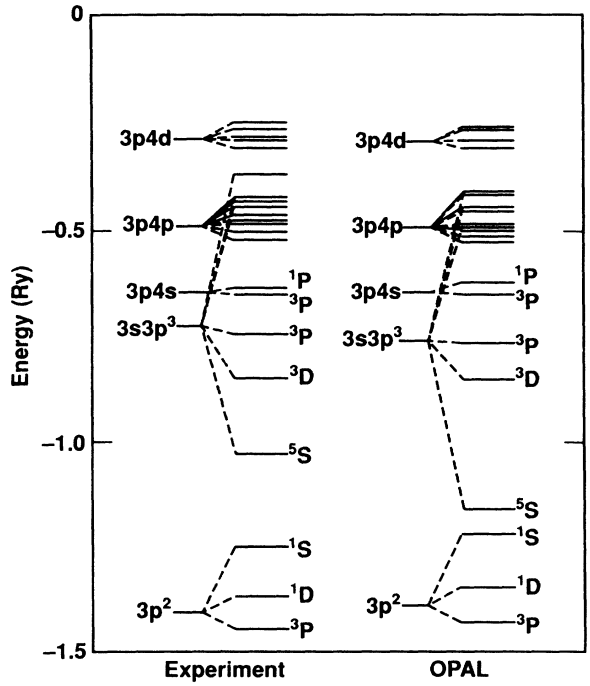


FIG. 5. Comparison of the configuration term structure for siliconlike phosphorus.

As mentioned earlier, one-electron binding energies for each subshell of a given configuration are calculated from a separate parent-configuration effective potential. Consequently, the set $\{\Psi_{nl}\}$ to be used in the configuration structure calculation is not uniquely defined. For simplicity, $\{\Psi_{nl}\}$ is taken from the parent associated with both initial and final configurations. To illustrate, consider

$$1s^2 2s 2p^2 \rightarrow 1s^2 2p^2 3p \ ,$$

where the running electron makes a $2s$ to $3p$ transition. The appropriate parent configuration is then $1s^2 2p^2$.

Figures 3 and 4 compare the calculated term structure with experiment[46] for carbonlike oxygen and neutral silicon. For few-times-ionized ions, or higher, the agreement with experiment is usually quite good and Fig. 4 is representative of the error. For some neutral atoms the term structure can be much more sensitive to configuration interactions and, in fact, neutral silicon is a worst-case situation. We show in Fig. 5 a comparison for siliconlike phosphorous where the agreement with experiment is considerably improved.

Model potential wave functions that reproduce ionization energies do not *a priori* guarantee accurate transition strengths since these quantities involve expectation values that weigh different regions of the radial wave functions. In addition, the photoionization cross sections require scattering states and again there is no *a priori* reason for the scattering wave functions to be accurate. Nevertheless, the effective potentials in OPAL seem to model the long-range and inner structure of atoms for both discrete and continuum states so that the resulting transition strengths are of similar quality as SCF calculations.

Sodiumlike systems are not complicated by the configuration structure and transition strengths reflect the quality of the one-electron wave functions. Table X compares the oscillator strengths for sodiumlike iron with results from Grant's relativistic SCF code.[56] Also displayed are the theoretical and experimental[45] transition energies. The photoionization cross section for neutral sodium is plotted and compared with results by Weisheit[57] in Fig. 6. Note that for both systems the OPAL

TABLE X. Oscillator strengths for sodiumlike iron. Comparison with Dirac-Hartree-Fock and experiment. Only open subshells are indicated.

| | Energy (eV) | | | $f$ value | |
|---|---|---|---|---|---|
| Transition | Expt. | Grant code | OPAL | Grant code | OPAL |
| 3*s*-3*p* | 36.1 | 35.7 | 34.6 | 0.397 | 0.376 |
| 3*s*-4*p* | 246 | 245 | 245 | 0.217 | 0.229 |
| 3*s*-5*p* | 337 | 336 | 336 | 0.067 | 0.070 |
| 3*p*-3*d* | 47.9 | 48.4 | 48.4 | 0.286 | 0.286 |
| 3*p*-4*s* | 195 | 195 | 196 | 0.065 | 0.063 |
| 3*p*-4*d* | 227 | 227 | 228 | 0.308 | 0.307 |
| 3*p*-5*s* | 294 | 294 | 295 | 0.0128 | 0.0125 |
| 3*p*-5*d* | 310 | 308 | 3100 | 0.098 | 0.098 |
| 3*d*-4*p* | 162 | 162 | 162 | 0.040 | 0.041 |
| 3*d*-4*f* | 187 | 186 | 187 | 0.925 | 0.930 |
| 3*d*-5*p* | 253 | 253 | 253 | 0.0064 | 0.0066 |
| 3*d*-5*f* | 266 | 264 | 266 | 0.170 | 0.171 |
| 4*s*-4*p* | 14.4 | 14.4 | 14.7 | 0.573 | 0.545 |
| 4*s*-5*p* | 106 | 106 | 105 | 0.230 | 0.242 |
| 4*p*-4*d* | 17.5 | 17.7 | 18.1 | 0.452 | 0.464 |
| 4*p*-5*s* | 84.1 | 84.6 | 84.8 | 0.110 | 0.107 |
| 4*p*-5*d* | 99.8 | 99.2 | 100 | 0.266 | 0.258 |
| 4*d*-4*f* | 7.4 | 7.3 | 7.2 | 0.110 | 0.102 |
| 4*d*-5*p* | 73.8 | 73.8 | 73.4 | 0.089 | 0.092 |
| 4*d*-5*f* | 86 | 85.8 | 85.6 | 0.724 | 0.725 |

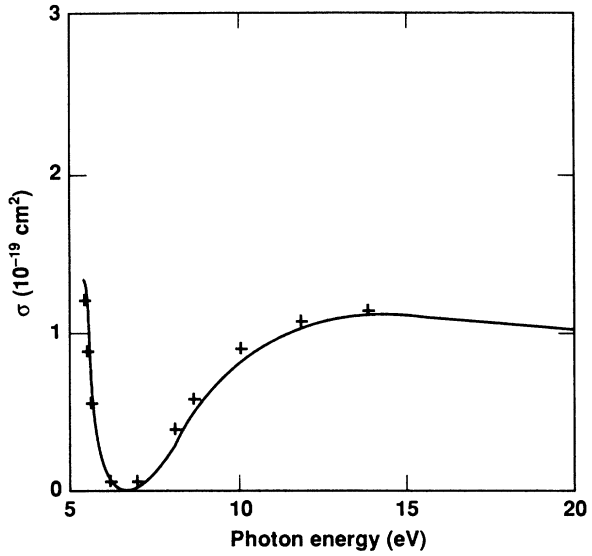


FIG. 6. Photoionization cross section for the 3*s* electron of neutral sodium: ——, OPAL; +, Weisheit.

results are comparable to the other theoretical calculations which suggest that the OPAL wave functions are of SCF quality.

Oscillator strengths for carbonlike oxygen are given in Table XI. The comparison is to Cowan's code, experimental data,[58,59] and some recent result by Pradham[10] using *R*-matrix theory. In general, the agreement between OPAL and Cowan is good. For the 2*s* and 2*p* transitions, both OPAL and Cowan agree poorly with the experiment. This transition is subject to pronounced configuration interaction which has been neglected when running the Cowan code and crudely included in OPAL by fitting the ionization energies to the experiment. The *R*-matrix calculation does include the configuration interaction and is in good agreement with experiment.

Finally, in Fig. 7 we show the 2*s* photoionization cross section for neutral lithium. A comparison to experiment[60] and calculations based on polarized orbitals[61] indicate that the OPAL result is failing at threshold where the cross section is sensitive to cancellation effects in the dipole matrix element. For higher photon energies, the OPAL results agree well with the theoretical calculation.

TABLE XI. Oscillator strength for carbonlike oxygen. Only open subshells are identified.

| Transition | Multiplet | OPAL | Cowan | Pradham | Experiment |
|---|---|---|---|---|---|
| $2s^2 2p^2$-$2s2p^3$ | $^3P$-$^3D$ | 0.185 | 0.206 | 0.107 | 0.11 |
| | $^3P$-$^3P$ | 0.130 | 0.142 | 0.137 | 0.14 |
| | $^3P$-$^3S$ | 0.254 | 0.268 | | 0.18 |
| | $^1D$-$^3D$ | 0.492 | 0.521 | | |
| | $^1D$-$^1P$ | 0.184 | 0.194 | | 0.23 |
| | $^1S$-$^1P$ | 0.617 | 0.652 | | 0.27 |
| $2p^2$-$2p3s$ | $^3P$-$^3P$ | 0.074 | 0.094 | 0.075 | 0.075 |
| | $^1P$-$^1P$ | 0.070 | 0.088 | | 0.064 |
| | $^1S$-$^1P$ | 0.062 | 0.078 | | |
| $2p^2$-$2p3d$ | $^3P$-$^3D$ | 0.487 | 0.448 | | |
| | $^3P$-$^3P$ | 0.163 | 0.155 | | |
| | $^1D$-$^1D$ | 0.091 | 0.085 | | |
| | $^1D$-$^1F$ | 0.524 | 0.494 | | |
| | $^1D$-$^1P$ | 0.006 | 0.006 | | |
| | $^1S$-$^1P$ | 0.566 | 0.531 | | |
| $2p3s$-$2p3p$ | $^3P$-$^3D$ | 0.340 | | 0.346 | 0.39 |
| | $^3P$-$^3S$ | 0.077 | | | 0.082 |
| | $^3P$-$^3P$ | 0.288 | | 0.276 | 0.28 |
| | $^1P$-$^1P$ | 0.139 | | | 0.15 |
| | $^1P$-$^1D$ | 0.489 | | | 0.51 |
| | $^1P$-$^1S$ | 0.123 | | | 0.13 |
| $2p3p$-$2p3d$ | $^3D$-$^3F$ | 0.493 | | | 0.51 |
| | $^3P$-$^3D$ | 0.349 | | | 0.42 |
| | $^3D$-$^3D$ | 0.096 | | 0.089 | 0.97 |
| | $^3P$-$^3P$ | 0.124 | | 0.104 | 0.14 |
| | $^3S$-$^3P$ | 0.614 | | | 0.59 |
| | $^1D$-$^1F$ | 0.413 | | | 0.41 |
| | $^1P$-$^1D$ | 0.458 | | | 0.59 |
| | $^1P$-$^1P$ | 0.203 | | | 0.19 |

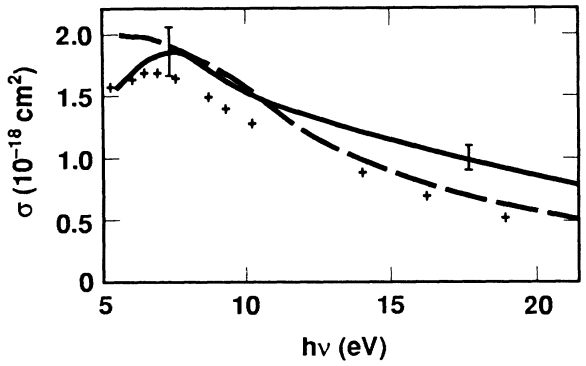


FIG. 7. Photoionization cross section for the 2*s* electron in the ground-state configuration of lithium: ——, experiment with error bars indicated (Ref. 60); — — —, OPAL; +, calculation Ref. 6.

## V. CONCLUSION

We have presented a parametric potential method for calculating the atomic data necessary in astrophysical equation-of-state and radiative opacity calculations. The effective potentials are analytic and consist of a Yukawa term for each occupied shell in the parent configuration plus a long-range Coulomb tail. The screening parameters were obtained by iteratively solving a spin-averaged Dirac equation until the ground-state eigenvalue matched the experimental configuration-average ionization energy.

An important feature of the present work is that the screening parameters were fitted by a simple function and are available for all ion stages of elements through the zinc isoelectronic sequence. It is also important to note that effective potentials can be rescaled for orbital-angular-momentum dependence and used to obtain the ionization energies of all states available to the running electron, including scattering states.

The vast majority of the transitions that arise in an opacity calculation involve an excited parent configuration. A prohibitively complicated procedure would be to make a table of coefficients similar to Table I for each of these excited parents. Furthermore, it would be hampered by insufficient experimental data. Instead, we were able to rescale the ground-state screening parameters to form new effective potentials for the excited parent configurations.

The results were compared to experiment and SCF calculations. For the configuration-average ionization energies, the agreement with experiment is better than a few percent. The configuration term structure, oscillator strengths, and photoionization cross sections are comparable with single-configuration SCF calculations. Although the method has been carefully tested through atomic number 30, preliminary results indicate that the method can be used at least through atomic number 40 and the rubidium isoelectronic sequence.

## ACKNOWLEDGMENT

The work was performed under the auspices of the U.S. Department of Energy by the Lawrence Livermore National Laboratory under Contract No. W-7405-ENG-48.

## APPENDIX A: EMPIRICAL FITS TO $\tau$

Section III A described how the screening parameters in Table I were determined. The resulting effective potential is used to calculate the energy for all excited states having the same $l$ as the ground state. A factor, $\tau$, to adjust the effective potential for changes in angular momentum of the running electron was introduced. In this appendix we summarize fits to the factor $\Theta(n)$ appearing in Eq. (6). These fits apply when $l > l_V$. When $l \leq l_V$ we set $\tau = 1$.

*Case a:* Ground-state parents with valence shell $K$

$$\Theta(1) = 0.048 + 0.000\,062(Z-3)^2 \ . \tag{A1}$$

*Case b:* Ground-state parents with valence shell $L$. If $\nu < 10$, then

$$\Theta(2) = 0.004 + 0.0019(Z-5)^2 \quad \text{for } l = 1 \ ,$$
$$\Theta(2) = 0.02 \quad \text{for } l \geq 2 \ . \tag{A2}$$

If $\nu = 10$, then $\Theta$ is set equal to zero.

*Case c:* Ground-state parent with valence shell $M$

$$\begin{aligned}
\Theta(3) &= -0.07 \quad \nu = 11 \text{ and } l = 1 \\
&= 0.07 \quad \nu = 11 \text{ and } l > 1 \\
&= 0.115 \quad \nu = 12 \\
&= 0.042 \quad \nu = 13 \\
&= 0.034 \quad \nu = 14 \\
&= 0.025 \quad \nu = 15 \\
&= 0.018 \quad \nu = 16 \\
&= 0.0125 \quad \nu = 17 \\
&= 0.21/\nu \quad \nu > 17 \ .
\end{aligned} \tag{A3}$$

## APPENDIX B: FITS TO THE VALENCE SHELL PROMOTION FACTOR EQ. (10)

Equations (7) and (8) give a scaling procedure for correcting the valence shell screening parameter for the

TABLE XII. Parameter values for Eq. (10).

| Electrons | $C_0$ | $G$ |
|---|---|---|
| 3 | 1.423 | 3.10 |
| 4 | 1.120 | 0.684 |
| 5 | 1.169 | −0.534 |
| 6 | 1.158 | −0.987 |
| 7 | 1.123 | −0.885 |
| 8 | 1.152 | −1.490 |
| 9 | 1.0 | −5.0 |

excitation of parent-ion electrons within the valence shell. Equations (9) and (10) give a method for improving the scaling procedure when experimental data is available. At present this is mostly limited to the $L$ shell. Table XII gives values to $C_0$ and $G$ for the $L$ shell. When a second $s$-shell electron is promoted to an open $p$ shell there is a small relaxation correction resulting from the first promotion. To approximately account for this effect, the value of $G$ [see Eq. (10)] is multiplied by a factor of 1.03.

## APPENDIX C: CONSTRUCTION OF ABSOLUTE ENERGY LEVELS

For equation-of-state purposes the relative values of configuration average total energies amongst excited parents are needed. For parents excited within the valence shell all energies can be referenced to the ground-state configuration by adding shift values. That is, the excited parent configuration energy $E_s$ is obtained from the ground-state configuration energy $E$ by

$$E_s(v,j,k)=E(v,j,k)+D(v,j)\ , \tag{C1}$$

where $v$ is the number of electrons in parent, $j$ is the index indicating the number of promotions in the valence shell (ground state $=1$, etc.), and $k$ is the index of eigenvalue ($1=1s$, $2=2s$, $3=2p$, . . . , etc.). The shift values $D$ are related to eigenvalues of configurations of higher ion stages by the formula

$$D(v,1)=0 \quad \text{for all } v\ , \tag{C2}$$

$$D(3,2)=E(2,1,p)-E(2,1,s)\ , \tag{C3}$$

$$D(4,2)=E(3,1,p)-E(3,1,s)\ , \tag{C4}$$

$$D(4,3)=E(3,2,p)-E(3,1,s)\ , \tag{C5}$$

while for $v=5-9$,

$$D(v,2)=E(v-1,2,p)-E(v-1,1,p) \tag{C6}$$

and for $v=5$ to 8,

$$D(v,3)=E(v-1,3,p)-E(v-1,1,p)\ . \tag{C7}$$

Similar formulas are available for the $M$ shell.

For the boronlike magnesium example of the next, the ionization limits of the ground-state parent and the parent with one valence shell excitation coincide with configurations having a common parent in the next higher ion stage. The shift in this case is given directly by the transition energy between the configurations of the higher ion stage. (Note that the formula for the shift values do not necessarily have a physical interpretation as transitions energies of higher ion stages.) The ionization limit of the doubly excited valence shell parent is an excited parent configuration of the higher ion stage. The shift relating the excited parents of the higher ion stage are obtained by considering the next higher ion stage, and so on. The procedure for boronlike magnesium is illustrated in Fig. 8.

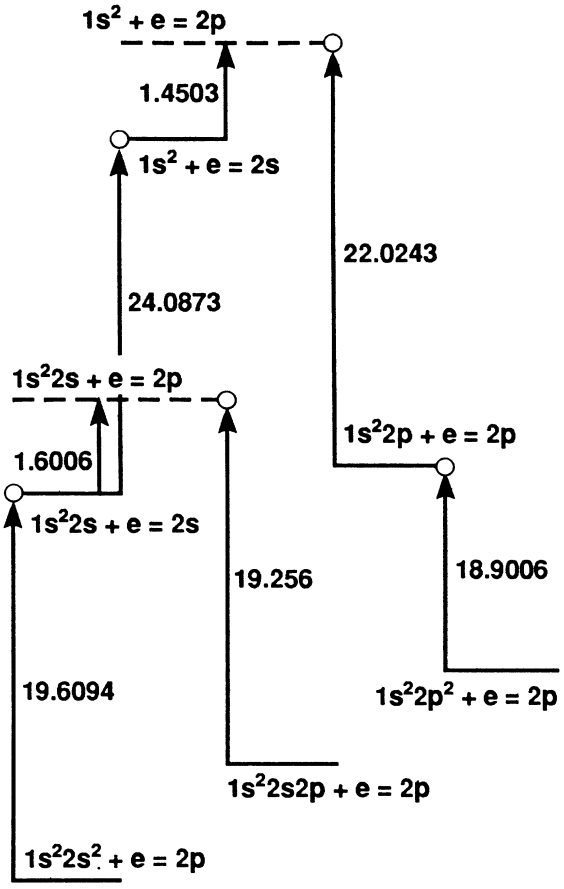


FIG. 8. Energy-level diagram for boronlike magnesium. Configurations are written in terms of a parent ( + ) ($e$, running electron orbital); ○, ionization limits for a given parent.

## APPENDIX D: REFINEMENT OF POTENTIALS FOR EXCITED PARENT CONFIGURATIONS

For excited parent configurations involving the excitation of inner-core electrons, the agreement between calculation and experiment can be improved by modifying the procedures outlined in Sec. III. In this appendix the following scalings are used to refine the screening parameters.

### 1. $K$-shell vacancies

The $\alpha_k$ parameter in Eq. (11) is modified according to

$$\alpha_k'=\alpha_k\left[1-c_q+\frac{c_q}{Z-v}\right]\ , \tag{D1}$$

where

$$c_q=0.32+0.0815(v-4),\quad 3\le v\le 9 \tag{D2}$$

$$c_q=0.32+0.024(v-12),\quad v>9\ . \tag{D3}$$

The valence shell screening parameter $\alpha_v$ is adjusted according to

$$\alpha_v'=\alpha_v\left[1+\frac{0.002\,08}{(v-3)^2}\right]\ . \tag{D4}$$

If the $K$ electron is promoted beyond the valence shell, then the modification given by Eq. (D4) will also affect the screening parameter for the parent electron above the valence shell through Eq. (16)

### 2. $L$-shell vacancies

In this case we improve the agreement with experiment by modifying only the $L$-shell screening parameter,

$$\alpha_L' = \alpha_L f_1(Z-10) f_2(Z-\nu) , \tag{D5}$$

where $f_1$ and $f_2$ depend on the net charge outside the closed $L$-shell and net ion charge, respectively,

$$f_1 = a + \frac{b}{Z-10} , \tag{D6}$$

$$f_1 = 1 - c_q + \frac{c_q}{Z-\nu} . \tag{D7}$$

If the promoted electron is from the $s$ subshell, then

$$\begin{aligned} &a = 1.04, \quad b = -0.16, \quad \nu < 18 \\ &a = 1, \quad b = 0, \quad \nu \geq 18 \\ &c_q = 0.16 + 0.0088(\nu - 12) . \end{aligned} \tag{D8}$$

If the promoted electron comes from the $p$ subshell, then

$$\begin{aligned} &a = 1.04, \quad b = -0.04, \quad \nu < 18 \\ &a = 1, \quad b = 0, \quad \nu \geq 18 \\ &c_q = 0.08 + 0.072(\nu - 12) . \end{aligned} \tag{D9}$$


[1] J. N. Bachall, W. F. Huebner, S. H. Lubou, P. D. Parker, and R. K. Ulrich, Rev. Mod. Phys. **54**, 767 (1982).

[2] N. R. Simon, Astrophys. J. Lett. **260**, L87 (1982).

[3] *Solar Seismology from Space: A Conference at Snowmass, Colorado,* edited by R. K. Ulrich, J. Harvey, E. J. Rhodes, Jr. and J. Toomre (Jet Propulsion Laboratory, Pasadena, CA, 1984).

[4] C. A. Iglesias, F. J. Rogers, and B. G. Wilson, Astrophys. J. Lett. **322**, L45 (1987).

[5] B. F. Rozsnayi, Phys. Rev. A **5**, 2 (1972).

[6] R. D. Cowan, *The Theory of Atomic Structure* (University of California, Berkeley, 1981).

[7] W. F. Huebner, in *Physics of the Sun,* edited by P. A. Sturrock (Reidel, Dordrecht, 1986), Vol. 1, p. 33.

[8] W. F, Huebner, A. L. Merts, N. H. Magee, and M. F. Argo, *Astrophysical Opacity Library,* Los Alamos Scientific Laboratory Manual No. LA-6970-M, 1977 (unpublished).

[9] M. J. Seaton, J. Phys. B **14**, 6363 (1987).

[10] A. K. Pradham, Phys. Scr. **35**, 840 (1987).

[11] W. Dappen, L. Anderson, and D. Mihalas, Astrophys. J. **319**, 195 (1987).

[12] K. A. Berrington, P. G. Burke, K. Butler, M. J. Seaton, P. J. Storey, K. T. Taylor, and Y. Yam, J. Phys. B **14**, 6319 (1987).

[13] Y. Yam, K. T. Taylor, and M. J. Seaton, J. Phys. B **14**, 6399 (1987).

[14] Y. Yam and M. J. Seaton, J. Phys. B **14**, 6409 (1987).

[15] M. J. Seaton, J. Phys. B **14**, 6431 (1987).

[16] J. F. Thornbury and A. Hibbert, J. Phys. B **14**, 6449 (1987).

[17] J. A. Fernley, K. T. Taylor, and M. J. Seaton, J. Phys. B **14**, 6457 (1987).

[18] R. E. H. Clark and A. L. Merts, J. Quant. Spectrosc. Radiat. Transfer **38**, 287 (1987).

[19] A. Merts and J. Keady (unpublished).

[20] J. D. Talman, P. S. Ganas, and A. E. S. Green, Int. J. Quant. Chem. **13S**, 67 (1979).

[21] J. D. Talman and W. Shadwick, Phys. Rev. A **14**, 36 (1976).

[22] P. P. Szydlik and A. E. S. Green, Phys. Rev. A **9**, 1885 (1974).

[23] A. E. S. Green, D. Sellin, and A. Zachor, Phys. Rev. **184**, 1 (1969).

[24] J. W. Dareqych, A. E. S. Green, and D. Sellin, Phys. Rev. A **3**, 502 (1970).

[25] P. P. Szydlik and A. E. S. Green, Phys. Rev. A **9**, 1885 (1974).

[26] R. Garvey, C. Jackman, and A. E. S. Green, Phys. Rev. A **12** (1975).

[27] J. Purcell, G. Kutcher, and A. E. S. Green, Phys. Rev. A **2**, 107 (1970).

[28] P. Szydlik, G. Kutcher, and A. E. S. Green, Phys. Rev. A **10**, 1623 (1974).

[29] P. S. Ganas and A. E. S. Green, J. Quant. Spectrosc. Radiat. Transfer **13**, 1171 (1973).

[30] P. S. Ganas, J. Appl. Phys. **62**, 1 (1987); J. Quant. Spectrosc. Radiat. Transfer **20**, 461 (1978).

[31] P. S. Ganas, Physica **119C**, 337 (1983).

[32] P. S. Ganas and A. E. S. Green, J. Chem. Phys. **73**, 3891 (1980).

[33] M. Klapisch, Comput. Phys. Commun. **2**, 239 (1971).

[34] E. N. Lassettre, J. Chem. Phys. **83**, 1709 (1985).

[35] J. Daudey and M. Berrondo, Int. J. Quantum. Chem. **19**, 907 (1981).

[36] F. Salvat, J. Martinez, R. Mayol, and J. Parellada, Phys. Rev. A **36**, 467 (1987); J. Phys. B **20**, 6597 (1987).

[37] F. Rogers, Phys. Rev. A **23**, 1008 (1981).

[38] J. C. Slater, *Quantum Theory of Atomic Structure* (McGraw-Hill, New York, 1960), Vols. I and II.

[39] C. Fischer, *The Hartree-Fock Method for Atoms: A Numerical Approach* (Wiley, New York, 1977).

[40] W. C. Martin, R. Zalubas, and A. Musgrove, J. Phys. Chem. Ref. Data **14**, 751 (1985).

[41] W. C. Martin and R. Zalubas, J. Phys. Chem. Ref. Data **12**, 323 (1983); **10**, 159 (1981); **9**, 1 (1980); **8**, 817 (1979).

[42] J. Sugar and C. Corliss, J. Phys. Chem. Ref. Data **10**, 1097 (1981); **9**, 473 (1980); **8**, 865 (1979); **7**, 1191 (1978); **6**, 317 (1977).

[43] C. Corliss and J. Sugar, J. Phys. Chem. Ref. Data **10**, 200 (1981); **8**, 1 (1979); **8**, 1109 (1979); **6**, 1253 (1977).

[44] J. Reader and J. Sugar, J. Phys. Chem. Ref. Data **4**, 353 (1975).

[45] W. L. Wiese, Oak Ridge National Laboratory Report No. ORNL-6089/V4, 1985 (unpublished).

[46] C. Moore, *Atomic Energy Levels,* Natl. Bur. Stand. (U.S.) Circ. No. 467 (U.S. GPO, Washington, D.C., 1949), Vols. 1 and 2.

[47] S. Bashkin and J. Stoner, Jr., *Atomic Energy Levels and Grotian Diagrams* (North-Holland, Amsterdam, 1975), Vols. 1 and 2.

[48] S. Fraga, J. Karwowski, and K. M. S. Saxena, *Handbook of Atomic Data* (Elsevier, New York, 1976).

[49] M. N. Mirakhmedov and E. S. Parilis, J. Phys. B **21**, 775 (1988).

[50]R. D. Cowan and D. C. Griffin, J. Opt. Soc. Am. **66**, 1010 (1976).
[51]G.E. Bromage, Appleton Laboratory (United Kingdom) Report No. AL-R3, 1978 (unpublished).
[52]K. Sevier, At. Data Nucl. Data Tables **24**, 323 (1979).
[53]D. Shirley, R. Martin, S. Kowalczyk, F. McFeely, and L. Ley, Phys. Rev. B **15**, 544 (1977).
[54]K. Huang, M. Aoyagi, M. Chen, B. Craseman, and H. Mark, At. Data Nucl. Data Tables **18**, 244 (1976).
[55]R. D. Cowan, J. Opt. Soc. Am. **58**, 808 (1968).
[56]I. P. Grant, B. J. McKenzie, P. H. Norrington, D. F. Mayos, and N. C. Pyper, Comput. Phys. Commun. **21**, 207 (1986).
[57]J. Weisheit, Phys. Rev. A **5**, 1621 (1972).
[58]W. L. Wiese, M. W. Smith, and B. M. Glennon, *Atomic Transition Probabilities,* Natl. Bur. Stand. Ref. Data Ser., Natl. Bur. Stand. (U.S.) Circ. No. 4 (U.S. GPO, Washington, D.C., 1966), Vol. 1.
[59]M. W. Smith and W. Wiese, Astrophys. J. Suppl. **23**, 103 (1971).
[60]R. D. Hudson and V. I. Canter, J. Opt. Soc. Am. **57**, 651 (1967).
[61]A. K. Bhatia, A. Temkin, and A. Silver, Phys. Rev. A **12**, 2094 (1975).